ELSEVIER

International Journal of Pharmaceutics 194 (2000) 21–38

international journal of pharmaceutics

www.elsevier.com/locate/ijpharm

# Formation of HDL-like complexes from apolipoprotein A-$I_M$ and DMPC

Malin Suurkuusk *, Satish K. Singh [1]

*Department of Pharmaceutical Technology, Pharmacia & Upjohn AB, SP 19-5, S-112 87 Stockholm, Sweden*

Received 19 April 1999; received in revised form 17 August 1999; accepted 2 September 1999

**Abstract**

Conditions for the preparation of reconstituted high density lipoproteins (HDLs) by incubation of the synthetic lipid dimyristoylphosphatidylcholine (DMPC) and recombinant apolipoprotein A-$I_M$ have been investigated as a function of ratio of incubation lipid to protein, incubation temperature and the lipid form (multilamellar (MLV) or small unilamellar (SUV) vesicles). The size distributions of the resultant lipid-protein complex particles from various incubations have been evaluated by native gel electrophoresis. Structural changes of the protein after incorporation into these complex particles have been estimated by CD. Thermal characteristics of the particles has been examined by DSC and correlated with CD results. Titration calorimetry has been used to obtain interaction parameters based on a simplified binding model. It is hypothesized that the major enthalpic step in the production of rHDLs is the primary association step between protein and lipid vesicles. It has been shown that by raising the temperature and incubation ratio, the formation of rHDL particles can be directed towards smaller size and a narrower size distribution. The results have been described on the basis of a model where formation of discoidal particles requires prior saturation of vesicle surface area by adsorbed protein, thus explaining differences between particles formed from MLVs and SUVs. 

*Keywords:* Apolipoprotein A-$I_M$; Reconstituted lipoprotein; Phospholipid–protein complex; Differential scanning calorimetry; Titration calorimetry; Circular dichroism

## 1. Introduction

Apolipoprotein A-I (apo A-I) is the major protein component in high density lipoproteins (HDL). One major function of HDLs is the transport of cholesterol from peripheral tissue to the liver for elimination, a process called 'reverse cholesterol transport' (RCT) (Glomset, 1968). HDL acts by being an effective acceptor of cellular cholesterol and by being a potent activator of

* Corresponding author. Present address: Thermometric AB, Spjutvägen 5A, SE-175 61 Järfälla, Sweden. Fax: +46-8-56472220.

*E-mail address:* malin.suurkuusk@thermometric.se (M. Suurkuusk)

[1] Present address: Pharmacia & Upjohn Inc., Kalamazoo, MI 49001, USA.

0378-5173/00/$ - see front matter 
PII: S0378-5173(99)00312-9

the enzyme lecithin cholesterol acyl transferase (LCAT), a key enzyme in the cholesterol metabolism (Meng et al., 1993). HDL is believed to have a protective role in the development of atherosclerosis due to this function (Gordon and Rifkind, 1989). HDL consists of a group of heterogeneous lipoprotein particles of distinct sizes and form; flat discoidal complexes with only protein and polar lipids (nascent HDL) and spherical complexes having a core of nonpolar lipids (mature HDL) (Fielding and Fielding, 1995).

Apo A-I is a 28 kDa protein consisting of 243 amino acids (Brewer Jr et al., 1978) arranged in repeating units of 11 or 22 amino acids, which are believed to form antiparallel amphiphatic α-helices interrupted by β-turns at glycine or proline residues (Segrest et al., 1992). This gives apo A-I a high α-helical content and a globular form when not associated with lipids. In the presence of phospholipids, the protein forms discoidal complexes from bilayers, with the α-helices coating the edges running from side to side of the disc. These disciodal complexes resemble nascent HDL particles (Wald et al., 1990) and are called reconstituted HDL (rHDL). The number of α-helices on the edges is dependent on the size of the particles with six, seven or eight α-helices per protein being accommodated on the edges. The α-helix content of the protein increases as a consequence of association with the lipid.

Apo A-I has been extensively investigated, along with the phospholipid-complexes and the complexation reaction. Dimyristoylphosphatidylcholine (DMPC) is the most commonly used lipid because of its 'fast' complexation reaction with the protein. Reaction rate has been found to be fastest at the gel to liquid-crystalline phase transition temperature ($T_c$) of the lipid (Swaney, 1980; Swaney and Chang, 1980). The initial ratio of lipid to protein in the incubation mixture is also an important parameter of the complexation reaction with different sized complexes being formed at different ratios; usually a distribution of particle sizes is obtained. The higher the ratio (lipid:protein) the larger the sizes of the complex particles formed (Jonas et al., 1980). The size of the particles is also dependent on whether the incubation is made with multilamellar vesicles (MLVs) or small unilamellar vesicles (SUVs).

Structure and function studies, using computer modeling (Phillips et al., 1997), by examination of deletion mutants (Davidson et al., 1996; Frank et al., 1997; Rogers et al., 1997, 1998) and point mutations (Laccotripe et al., 1997), or by studying the individual α-helices (Palguanachari et al., 1996), have provided new insights into the interaction between the protein and lipids, and into how the lipoprotein interacts with other proteins, receptors and lipoproteins.

A natural molecular variant of this protein has been found in a family in Italy. This variant has a single amino acid substitution at position 173, where an arginine is replaced with a cystein and the resulting protein exists as a disulfide-linked homodimer (Weisgraber et al., 1983). This substitution occurs in one of the α-helices and thus facilitates interaction between α-helices, which affects the secondary as well as the tertiary structure and thereby the lipid binding properties of the protein (Calabresi et al., 1994). Studies comparing apo A-I and this dimeric variant show that association rates do not differ between the proteins, however it has been shown that the discoidal particles formed between the dimer and phospholipids are not as heterogeneous in size distribution as particles with normal apo A-I, which implies that the disulfide linkage restricts the possible range of protein conformations (Calabresi et al., 1997). The variant protein is named apolipoprotein A-$I_{Milano}$ (apo A-$I_M$) and carriers of this protein have low prevalence of developing atherosclerosis (Franceschini et al., 1987). This implies that the protein may have a different RCT-effect than normal apo A-I. Since a single amino acid substitution has such a profound effect on the function of HDL, it is of great interest to study both the complexation reaction and the physical properties of the particles formed, and compare them with the normal protein and its lipid complexes.

Studies have shown that infusion of HDL plasma fraction can cause regression of atherosclerotic lesions in cholesterol-fed rabbits (Badimon et al., 1990). This and the low prevalence of atherosclerosis in carriers of apo A-$I_M$

suggest a pharmaceutical application of rHDL particles in the treatment of this disease. This concept has been demonstrated in animal studies (Andersson, 1997).

The aim of this study was to identify and understand conditions for the reproducible formation of rHDL particles based on a process that could be scaled-up for producing these particles for pharmaceutical applications. The starting point was small homogeneous particles, since small HDL particles have been considered the most effective cholesterol scavengers, and homogeneous particles are much more easy to characterize. The complexation between dimeric apo A-$I_M$ and DMPC in an incubation mixture has been examined as a function of lipid form (MLV or SUV), temperature and molar ratio lipid:protein. The results have been compared to that from normal apo A-I. The resultant mixtures of particles have been studied with differential scanning calorimetry (DSC) for thermal behavior, circular dichroism (CD) for change in secondary structure and native gel electrophoresis (n-PAGE) for sizes and relative amounts of the particles and presence of free protein. Isothermal titration calorimetry (ITC) has also been employed on the system and the data evaluated in a simplified binding model as a basis for discussion.

## 2. Materials and methods

### 2.1. Protein

Apolipoprotein A-$I_M$ was expressed in *E. Coli* and purified as described elsewhere (Calabresi et al., 1994). The protein used was produced for toxicological studies and was dissolved in water for injection at a concentration of 22.5 mg/ml according to a SDS-gelfiltration method. 93% of the protein exists as dimer 3.5% as monomer and 3.5% as multimers. Lyophilized wild-type apolipoprotein A-I (purity > 96%) was purchased from Biogenesis Ltd. (Dorset, England) and used without further purification.

Protein was diluted in 10 mM sodium-phosphate buffer at pH 7.4 to an approximate concentration of 10 mg/ml. 15 ml protein solution was put in a 15 ml slide-A-lyzer cassette with a molecular weight cutoff at 10 kDa (Pierce, Rockford, IL, USA). Protein was dialyzed against 2 l buffer with gentle stirring for at least 4 h at 4°C, before changing the buffer and left over night. After dialysis, the protein concentration was determined with the Lowry method (Protein Assay kit P5656, Sigma Diagnostics, St. Louis, MO, USA). The apo A-$I_M$ was frozen in 2 ml aliquots and the buffer against which it was dialyzed was also frozen in 40 ml aliquots.

### 2.2. Preparation of lipid vesicles

Dimyristoylphosphatidylcholine (DMPC) was obtained from Chemi spA, Italy (with a stated purity of > 99%). DMPC was mixed with the same buffer as the protein was dialyzed against. The mixture was vigorously shaken at 25°C, to produce MLVs. To produce SUVs, the MLV-dispersion was sonicated at level 3 for $3 \times 10$ min using a microtip (Sonicator Misonic, Misonic Inc. Farmingdale, NY, USA), and subsequently centrifuged for 20 min at 5000 rpm to remove residual MLVs and titanium particles eroded from the sonication tip. The SUVs were examined with dynamic light scattering (Zetamaster S, Malvern Instruments Ltd. Worcestershire, UK) to confirm size and homogeneity. Size by number was 25 nm $\pm$ 15 nm. The vesicles were kept at 25°C (above the $T_c = 24.3$°C for DMPC) and used within 2 days. The concentration of DMPC after sonication and centrifugation was determined with an enzymatic colorimetric test from Boehringer Mannheim (MPR 2 691 844).

### 2.3. Preparation of lipid–protein complexes

Lipid–protein complexes were prepared by the incubation method by simply mixing the protein and vesicle preparations with gentle stirring. All incubations were performed over 24 h at 25°C unless otherwise stated. At least triplicates of every incubation were done. All molar ratios between lipid and protein are calculated with the molecular weight of the protein dimer. The complexation process between lipid and protein was examined for incubation ratios ranging from 10:1 to 4000:1.

### 2.4. Characterization of DMPC–apo A-$I_M$ complexes

Native polyacrylamide gel electrophoresis (n-PAGE) was used to determine the sizes of complex formed between lipid and protein. Electrophoresis was run using the X Minicell-II from Novex (San Diego, CA, USA). Precasted Novex 4–20% polyacrylamide gels were run for 5 h 125 V (LKB 2297 Microdrive 5 Constant Power Supply) under non-denaturing conditions. Gels were stained with Coomassie Brilliant Blue R-250 and dried between cellophane sheets. The gels were thereafter scanned using the Sharp JX-325 scanner connected to a computer with the program Image-Master 1.10 (Pharmacia Biotech, Uppsala, Sweden). Thyroglobulin (17.0 nm), ferritin (12.2 nm), catalase (10.4 nm), lactase dehydrogenase (8.2 nm) and albumin (7.1 nm) were used as size standards (High molecular weight calibration kit, HMW Electrophoresis Calibration Kit, Pharmacia Biotech, Uppsala, Sweden).

For sizing of complexes obtained from incubations at temperatures above $T_c$ of the lipid (30 and 40°C), all gels and solutions were pre-warmed to the incubation temperature in order to prevent changes in the particles when loading and running the gels. Electrophoresis was subsequently performed at the incubation temperature for the same reason.

Differential scanning calorimetry (DSC) was performed on a MC2 Ultrasensitive Differential Scanning Calorimeter (Microcal Inc. Northampton, MA, USA). Data were collected by the MC-2 DSCITC Software supplied with the instrument. Scans were made between 10 and 95°C at a scan rate of 60°C/h. Protein, vesicles and rHDL particles were prepared as described above, degassed, filled into the fixed 1.2 ml cell and pressurized under nitrogen. All scans were made with the corresponding buffer in the reference cell. A buffer versus buffer scan was also made each day and used as control and reference. The lowest concentration at which protein transitions could be detected was 7 mg/ml. Consequently protein concentration was kept constant while the lipid concentration was adjusted to achieve the desired ratio. At least two samples of each ratio were run. Data analysis was made with the Origin™ software (Microcal Software Inc. Northampton, MA, USA).

FarUV-CD spectra were run on the Jasco J-720 Spectropolarimeter (Jasco Corporation, Tokyo, Japan) equipped with peltier element (PTC-348 WI) for temperature control. Instrument control and data collection was done with the J-700 software. Wavelength-scans were made between 250 and 190 nm, at a scan rate of 20 nm/min, using 0.1 cm quartz cuvettes. Three scans of the same solution were averaged. Scans were made on pure protein as well as on complexes produced from incubations at different ratios. Protein concentration was kept constant around 0.1 mg/ml. CD-spectra were also measured as function of temperature. Wavelength scans were taken every 10° starting at 10 up to 80°C. The temperature scan rate was 60°C/h. While changing the temperature, the ellipticity at 222 nm was monitored continuously. Buffer scans were run every day, and subtracted from the protein and rHDL scans. The CD-signal was converted to molar mean residue ellipticity, $[\theta]$, expressed in degrees·cm$^2$ dmol$^{-1}$ and calculated as

$$[\theta]*(\theta)_{obs} \cdot 115/(10 \cdot l \cdot c) \quad (1)$$

where $(\theta)_{obs}$ is the observed ellipticity in degrees, 115 is the mean residue molecular weight of the apo A-$I_M$, $l$ is the optical path-length in cm and $c$ is the protein concentration in g/ml.

Titration experiments (ITC) were performed in the Thermal Activity Monitor (Thermometric AB, Järfälla, Sweden), equipped with nanowatt-amplifiers and 2-ml titration cells. Experiment control and data collection was done with the Digitam Software (Scitech Software, Järfälla, Sweden). The calorimeters were calibrated electrically using both static and dynamic calibrations. 800 ml of a DMPC solution (2–190 mg/ml) was placed in the titration cell. After equilibration of the system, a protein solution (2–7 mg/ml) was titrated into the cell in 15 ml aliquots over 30 s. At least 15 injections were made. Once the heat signal returned to the baseline level after an injection, a 5 min baseline was collected before the next injection. Since the reaction rates were slow, the time period between injections was at least 45

min. The system was stirred at 80 rpm with a gold propeller. All measurements were performed at 25°C.

## 3. Results

### 3.1. Size-distribution of lipid–protein complexes

The size-distribution data for complexes produced in the various incubations are obtained in terms of percentage of total protein in each particle size band as exemplified in Figs. 1 and 2. The bands observed in native gel electrophoresis of DMPC–apo A-$I_M$ complexes were sized as 7.4 nm for the free protein (6.5 nm for free apo A-I) and 8.2, 10, 11, 12 nm for the rHDL discoidal particles. Complexes larger than 12 nm have been grouped together and labeled as '$>12$ nm' due to the lower resolution. Since staining is specific for protein and the total protein concentration is known, the amount of free protein and lipid-bound protein in each band could be estimated; lipid concentration in the band is however not quantifiable. Staining also showed protein in the well in many cases, which is only possible if this protein is associated to vesicles too large to migrate into the gel. These association complexes are referred to as lipid–protein vesicular complex in the text. The amount of protein in these lipid–protein vesicles left in the well has been estimated and labeled as 'well' in Figs. 1 and 2. The standard deviation for the estimation of protein in the bands are mostly less than 10% ($n=3$); due to some difficulty in resolving the 10 and 11 nm bands, somewhat higher standard deviations where occasionally seen here.

Incubations at 25°C of apo A-$I_M$ with MLVs and SUVs at various molar ratios (100, 200, 400 and 800 to 1) results in a heterogeneous mixture of complexes (Fig. 1). In general, incubations with MLVs were found to yield a more homogenous mixture of complex particles than the incubations with SUVs. The predominant size of particles obtained from MLVs is 11 nm, the fraction of which decreases with increasing ratio while the fraction of larger particles increases. The particles formed at an incubation ratio of 100:1 (the only ratio with free protein remaining) however include a large 8 nm fraction. In incubations with SUVs, the higher the ratio the larger the proportion of larger particles formed. At the lower ratios (100 and 200 to 1) free residual protein is observed, unlike at the higher ratios. Incubations with apo A-I at 25°C (molar ratios 50, 100 and 200 to 1) show no major difference when performed with either MLVs or SUVs. The 10 and 11 nm complexes are predominant with the higher ratios leading to more 11 nm particles. All ratios have unassociated protein, the MLV incubations somewhat more than SUVs (not shown).

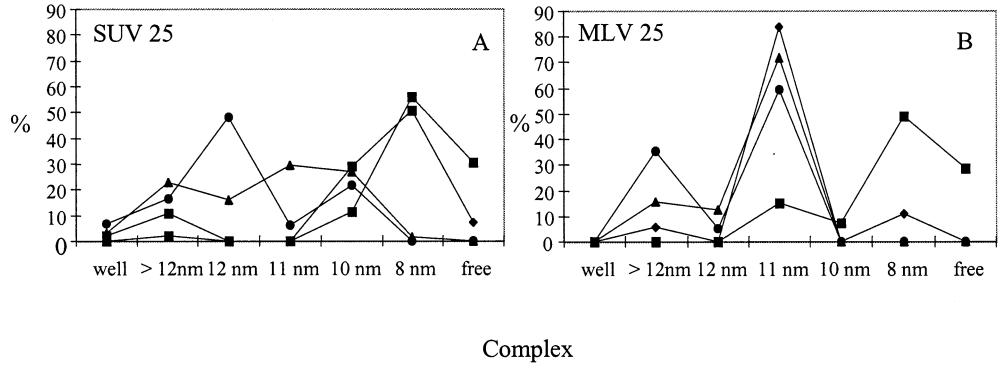


Fig. 1. Percentage of total protein (apo A-$I_M$) obtained in each band (corresponding to particle size distribution) on analysis of incubation mixtures by n-PAGE. Incubations have been made at various molar ratios of lipid:protein at 25°C (■, 100:1; ◆, 200:1; ▲, 400:1; ●, 800:1) with SUVs (A) and with MLVs (B).

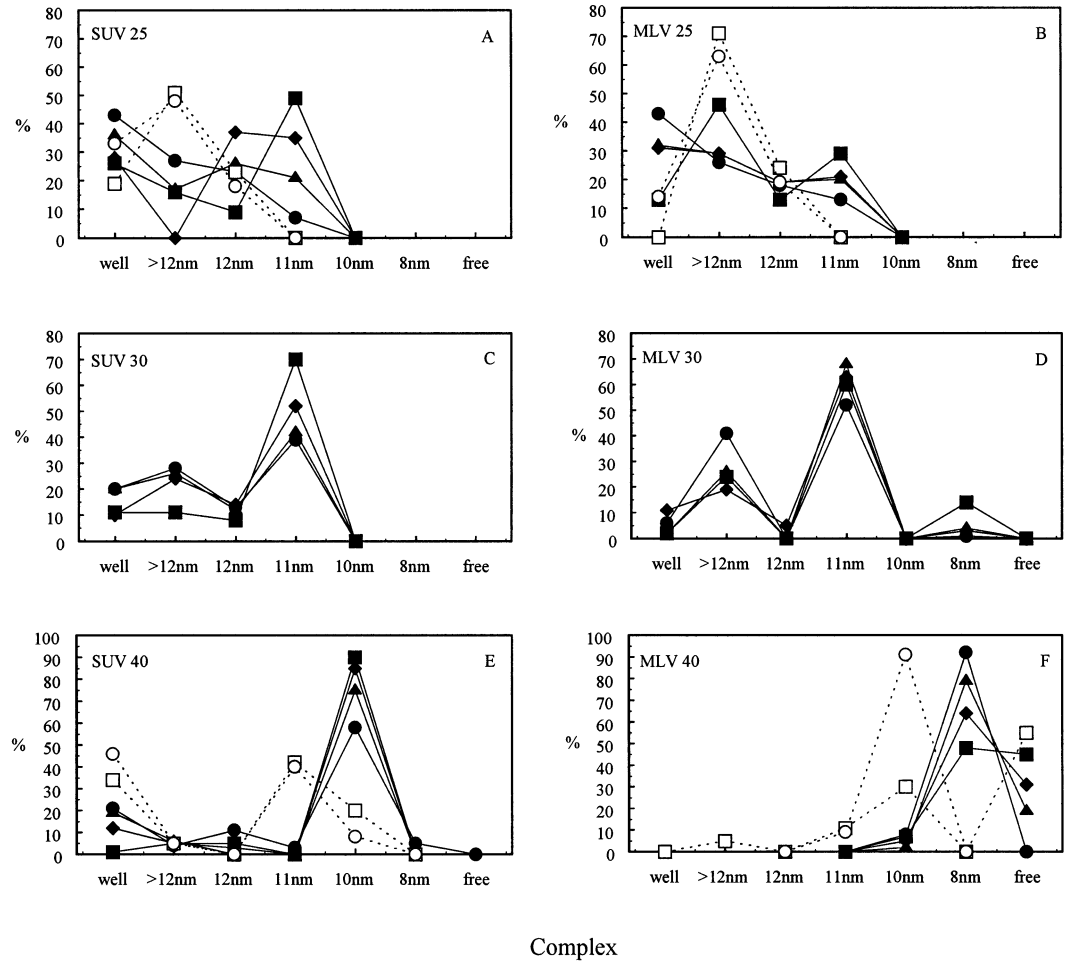


Fig. 2. Percentage of total protein obtained in each band (corresponding to particle size distribution) on analysis of incubation mixtures by n-PAGE. Incubations have been made at various molar ratios of lipid:protein (■, 500:1; ◆, 1000:1; ▲, 2000:1; ●, 4000:1) with SUVs at 25°C (A); 30°C (C); 40°C (E); and with MLVs at 25°C (B); 30°C (D); and 40°C (F). Closed symbols represent apo A-$I_M$, while open apo A-I.

The results from incubation of apo A-$I_M$ with lipid vesicles at high ratios and at various temperatures are shown in Fig. 2. At 25°C, apo A-$I_M$ forms mostly large complexes with both MLVs and SUVs. There is no free protein left in any of the incubations. The 11 nm particle is the smallest size formed, with the fraction of particles of this size decreasing as the ratio is increased. The same trend is observed with apo A-I, but the smallest complex formed is 12 nm. At 30°C with SUVs, the 11 nm particle is still predominant but the apo A-$I_M$ fraction in the well (lipid–protein vesicular complexes) decreases. The amount of 11 nm particles formed is dependent on the ratio, with the lower ratios giving more particles of this size. Incubations with MLVs also yield even smaller particles (8 nm) in addition to the 11 nm particles. There is less protein left in the well than with the SUVs at this temperature, but there is a high proportion of particles > 12 nm.

Incubation at 40°C results in particles that are quite homogenous. SUVs yield primarily 10 nm particles. There is a protein fraction left in the well, which increases with the ratio while the

fraction of 10 nm particles decreases. While small fractions of other complexes are also formed, the predominant size is 10 nm. For the MLV incubations on the other hand, the only complex formed is the 8 nm rHDL particle (with < 10% of the 10 nm particle). However there is a large fraction of unreacted protein too. The amount of 8 nm complex increases as the ratio increases, which is opposite of that observed from SUVs for the 10 nm particles. There is certainly free un-associated lipid left in the well, since the lipid is far in excess. In the case of MLVs a dispersion could be seen in the well at every temperature. With SUVs this could however not be visualized due to the small size of the vesicles. With apo A-I and SUVs the trend is the same, however there is a displacement towards larger sizes. MLVs and apo A-I at the lowest ratio result in a broad size distribution, but the highest ratio produces almost only 10 nm complex.

### *3.2. Thermal characterization of DMPC–apo A-$I_M$ complex*

Temperature scans with pure DMPC dispersion (MLV) show the characteristic transitions (Fig. 3a); a pre-transition is observed at 15°C and a main transition at 24°C as expected. A scan on DMPC SUVs was also made resulting in a more complex thermogram (data not shown; see Suurkuusk and Singh, 1998). The total transition enthalpy in MLVs is more than ten times larger than for SUVs. A DSC thermogram of the pure protein solution in buffer is shown in Fig. 3b. Two small peaks can be seen: the first at 31°C and the second at 52°C. On re-heating the protein after cooling, the first peak becomes smaller while the second remains unchanged. This was observed to be independent of the cooling-rate (not shown).

The thermograms from DSC runs on incubation mixtures with different ratios of DMPC MLVs: protein are shown in Fig. 4a. Three principal peaks are seen, the first of which is a broad one just below 30°C (peak I). This peak is small to non-existent at low ratios and grows rapidly with increasing ratios. At the higher ratios, sharp peaks corresponding to MLV pre- and main-transitions appear, overlapping with peak I. The second peak (peak II) is apparent at 52–55°C at the lowest ratios (10:1, 25:1), disappears at ratios 50:1 and 100:1, and then reappears at the higher ratios (200:1, 400:1). The third major peak (peak III) appears at higher temperatures and grows in size and shifts to lower temperatures (from 84 to 72°C) with increasing ratios.

In order to test reversibility of the thermal transitions, one of the incubation mixtures (ratio 50:1) was reheated twice. As shown in Fig. 4b, a peak corresponding to the DMPC main transition appears and grows with each reheating cycle, while peak III decreases in size at the same position. This suggests that heating to 95°C leads to generation of free phospholipid (vesicles) that do not completely re-complex within the time scale of the experiment; this free lipid apparently arises

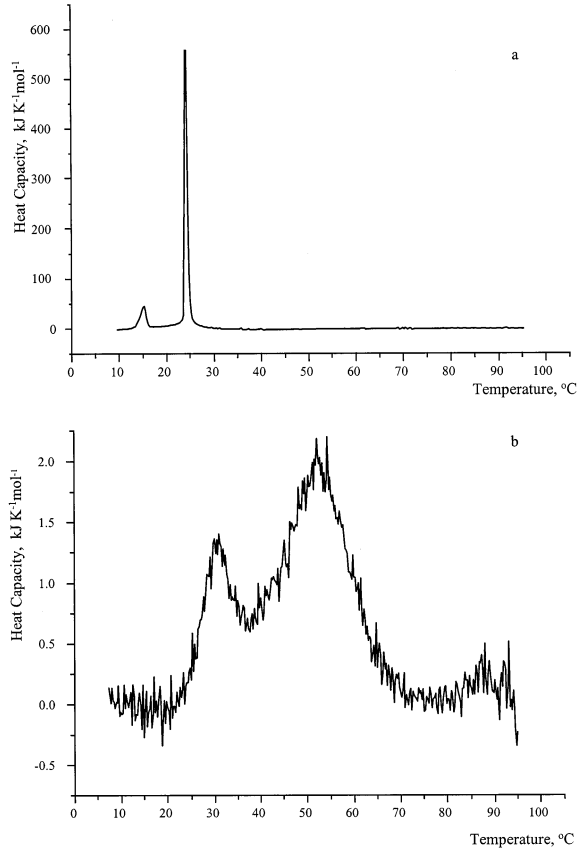


Fig. 3. Thermograms from DSC scans on (a) pure DMPC MLVs; and (b) pure protein.

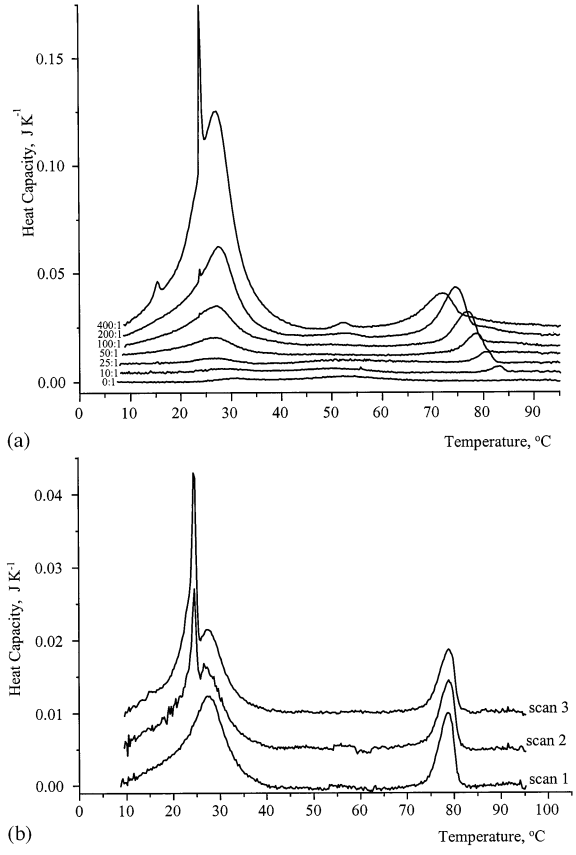


Fig. 4. Thermograms from DSC scans on lipid:protein complexes in incubation mixtures with MLVs. (a) Effect of various ratios of lipid to protein. The ratios have been obtained by keeping the protein concentration constant, while increasing the lipid concentration. No concentration corrections have been made on the scans. (b) Three consecutive heating scans on an incubation mixture of MLVs and protein at the ratio 50:1.

from that portion which ordinarily melts in peak III.

DSC data has been analyzed by first subtracting the corresponding buffer-reference thermograms. Thereafter, a (cubic connect) baseline was subtracted and a non-2-state function was fitted. From the fit, the transition midpoint (peak) temperatures and the total transition enthalpies were calculated. These results are summarized in Table 1.

Due to the difficulty in estimating the actual amount of material (lipid and/or protein) melting in each of the peaks, the total enthalpy for peaks I and III have also been recalculated on the basis of total lipid in the cell. This data has also been summarized in Table 1. The dependence of peak temperatures on the composition of the incubation mixture is shown in Fig. 5a; (has been indicated on the $x$-axis whether the incubation has been made with MLVs and/or SUVs). Peak temperatures for pure DMPC MLVs and for the pure protein itself are also shown for reference. Differ-

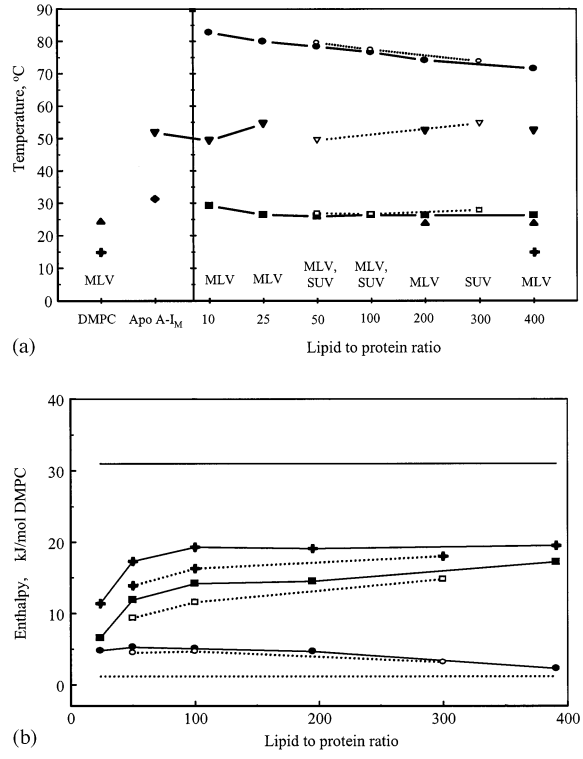


Fig. 5. Thermal characteristics of DMPC-Apo A-I$_M$ complexes. (a) Peak (if present) midpoint temperature as function of lipid:protein ratios for incubations with MLVs (closed symbols, —) and/or SUVs (open symbols, ---) as indicated on the $x$-axis: ■, peak I; ▼, peak II; and ●, peak III as identified in the text. The peak temperatures for DMPC MLVs and pure apo A-I$_M$ are also shown: +, DMPC pre transition; ▲, DMPC main transition; ◆, pure protein low temperature peak; ▼, pure protein high temperature peak. (b) Corrected heats for peak I and peak III as function of lipid:protein ratios with MLVs (closed symbols, —) and/or SUVs (open symbols, ---). +, Total heat for both peaks; ■, peak I; and ●, peak III. The upper straight lines is the main transition enthalpy for MLVs The lower dotted line is the total transition enthalpy for SUVs.

Table 1
Summary of results from the DSC experiments

| Ratio lipid to protein | DMPC pretransition | | | DMPC maintransition | | | Peak I | | | 1st protein | | | Peak II 2nd protein | | | Peak III | | |
|---|---|---|---|---|---|---|---|---|---|---|---|---|---|---|---|---|---|---|
| | $T_m$ (°C) | $\Delta H$ | | $T_m$ (°C) | $\Delta H$ | | $T_m$ (°C) | $\Delta H$ | | $T_m$ (°C) | $\Delta H$ | | $T_m$ (°C) | $\Delta H$ | | $T_m$ (°C) | $\Delta H$ | |
| | | (mJ) | (kJ/mol total lipid) | | (mJ) | (kJ/mol total lipid) | | (mJ) | (kJ/mol total lipid) | | (mJ) | (kJ/mol total protein) | | (mJ) | (kJ/mol total protein) | | (mJ) | (kJ/mol total lipid) |
| DMPC[a] | 15 | 93 | 5.1 | 24 | 570 | 31 | | | | | | | | | | | | |
| Apo A-$I_M$[b] | | | | | | | | | | 31 | 14 | 84 | 52 | 46 | 281 | | | |
| 10 MLV | | | | | | | 29 | 27 | 27 | | | | 49 | 29 | | 83 | 8 | 4.7 |
| 24 MLV | | | | | | | 26 | 24 | 6.6 | | | | 54 | 334 | | 80 | 18 | 4.8 |
| 50 MLV | | | | | | | 26 | 96 | 12 | | | | | | | 78 | 43 | 5.3 |
| 50 SUV | | | | | | | 27 | 76 | 9.0 | | | | 49 | 3 | | 80 | 36 | 4.5 |
| 100 MLV | | | | | | | 26 | 232 | 14 | | | | | | | 77 | 82 | 5.1 |
| 100 SUV | | | | | | | 26 | 188 | 12 | | | | | | | 77 | 76 | 4.7 |
| 195 MLV | | | | 24 | 2.8 | 0.1 | 26 | 460 | 15 | | | | 52 | 8 | | 74 | 148 | 4.7 |
| 300 SUV | | | | | | | 28 | 718 | 15 | | | | 55 | 17 | | 74 | 157 | 3.2 |
| 391 MLV | 15 | 5.4 | 0.1 | 24 | 48 | 0.7 | 26 | 1094 | 17 | | | | 52 | 6 | | 71 | 146 | 2.3 |

[a] MLVs.
[b] Protein in buffer.

ences between incubations with MLVs and SUVs are only seen in size of peak II; peak temperatures for I and III show no difference as far as incubation with MLVs or SUVs is concerned.

Fig. 5b shows the enthalpies of peak I and III (calculated per mol total DMPC) from the various incubations with either MLVs or SUVs as in Fig. 5a. Assuming that all the lipid melts either in peak I or III, a sum of the lipid transition enthalpy in the system can be made, assuming that the heat capacity for the lipid does not change in the temperature interval studied here. The total lipid transition enthalpy (peak I + peak III) has been plotted in Fig. 5b and shows that while enthalpy of peak I increases and that of III decreases with increasing ratio, their sum reaches a plateau at and above a ratio of 100:1. This observation holds for the incubations with MLVs, while the data for SUVs indicates the same trend. Also shown in Fig. 5b are the main transition enthalpies for pure DMPC MLVs and SUVs. It is clearly apparent that the lipid molecules in the incubation mixture exist in a higher energetic state than those in MLVs although not as high as the molecules in SUVs.

### 3.3. Circular dichroism of DMPC–apo A-$I_M$ complexes

The amount of α-helical structure in the protein has been approximated by the expression

$$\%\ \alpha\text{-helix} = -100*([\theta]_{222\ nm} - 3000)/39000 \qquad (2)$$

This equation can be used assuming that the only structural motifs are random coil and α-helix (Pownall et al., 1977). The ellipticity at 222 nm decreases as the lipid to protein ratio increases, as is expected since conformation changes are known to occur when the protein binds to lipids. The α-helix values are summarized in Table 2. The α-helix content is similar irrespective of whether the particles are incubated from MLVs or SUVs. The values are of the order of previously published results (Calabresi et al., 1994), and increase with increasing ratio over the range examined.

The α-helical content of pure protein and of complexed-protein at various ratios is shown in Fig. 6 as a function of temperature. This data has been plotted for incubations with SUVs; MLVs resulted in similar trends and values. The pure protein shows two distinct changes in slope of % α-helix versus temperature: the first between 20 and 30°C and the second around 60°C. These temperatures correspond well with the DSC peaks for pure protein (Fig. 5a) and are indicated by circles in Fig. 6. The α-helix content of protein after incubation with different amounts of lipid is also shown in this figure. Slight changes in the slopes of the curves are again observable with temperature. The 50:1 incubation mixture shows a steady decrease in α-helix content with increasing

Table 2
Amount of α-helix determined from the mean residue weight ellipticity at 222 nm

| Lipid to protein ratio | SUV | MLV |
|---|---|---|
| | % α-Helix | % α-Helix |
| 50:1 | 61 | 63 |
| 100:1 | 65 | 69 |
| 200:1 | 72 | 79 |
| 400:1 | 81 | 82 |
| Apo A-$I_M$ | 60 | % α-Helix |

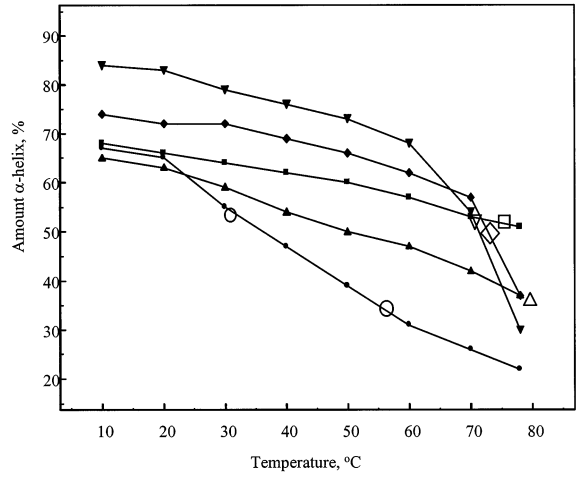


Fig. 6. α-Helical content of apo A-$I_M$ calculated from the ellipticity at 222 nm as a function of temperature and lipid:protein ratio in incubation mixtures. ●, Pure protein; ▲, 50:1; ■, 100:1; ◆, 200:1; and ▼, 400:1. The empty symbols are the corresponding midpoint temperatures from DSC measurements for the same ratios.

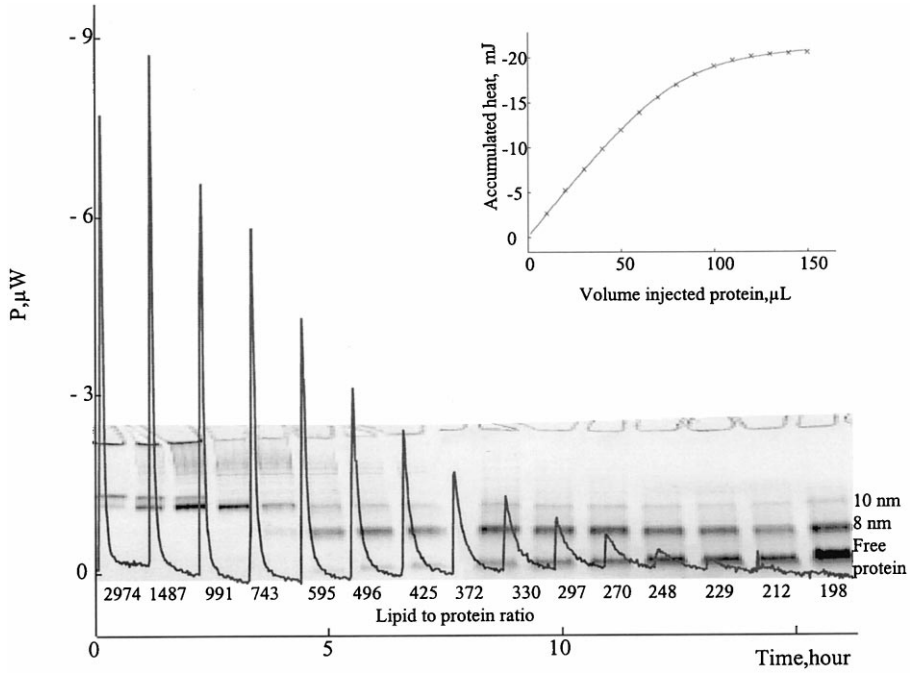


Fig. 7. Microcalorimetric heat flow curve for titration of protein into a MLV dispersion. As an inlay in the figure is the total heat per mole injected protein (kJ/mol) plotted as a function of the protein/lipid ratio in the vessel. (x) is the experimental value and (--) is the calculated curve from the model used (Eq. (7)). In the background are the n-PAGE gels, run from incubations performed at ratios corresponding to the injections in the foreground.

temperatures. The DSC peak III temperature for this ratio is indicated on this plot and also lies just beyond the range studied. No drastic drop in α-helical content could be detected in the temperature interval 10–80°C by CD; the DSC peak III temperature is 77°C (Table 1). The 200:1 incubation mixture starts from a higher initial α-helix level but shows a more rapid drop in α-helix content with temperature and a dramatic drop above 70°C, corresponding well with DSC peak III temperature of 72°C. Similarly, the 400:1 mixture leads to a higher content of less stable α-helices that show a rapid melt above 60°C; the corresponding DSC peak III temperature is 71.5°C (Table 1).

### 3.4. Titration calorimetry of DMPC vesicles with apo $A\text{-}I_M$

Based on the observable heat flow after each injection requiring the use of injection periods up to 50 min, it can be construed that the lipid–protein complexation is a slow process. The reaction with MLVs ( ~ 40 min) were however found to be somewhat faster than with the SUVs ( ~ 50 min).

A typical titration curve into MLVs is shown in Fig. 7. The area under each peak is proportional to the fraction of protein that has reacted,

$$Q = [ML]/[M]_{\text{total}} \cdot \Delta H \cdot x_i \tag{3}$$

where $x_i$ is the total amount protein injected in the $i$th injection.

Integrated injection heat flow values ($Q_i$) were fitted to a 1:1 model using:

$$M + L \rightarrow ML \tag{4}$$

with

$$K = [ML]/([M] \cdot [L]) \tag{5}$$

and

$$[M]_{\text{total}} = [M] + [ML] \tag{6}$$

$$Q = (K \cdot [L]_i \cdot \Delta H)/(1 + K \cdot [L]_i)x_i \quad (7)$$

A non-linear least square analysis was performed to fit Eq. (7) to the ITC data and recover $K$ and $\Delta H$. The results of the fit are shown as an inlay in Fig. 7. The total amount of protein in the cell was not used as an input in the least squares analysis. Instead, a model based 'protein concentration, $[M]_{total}$' was calculated from the $K$ and the total lipid concentration. The actual protein concentration was then divided by this model-based 'protein-concentration' to recover the value '$n$' where $n$ can be treated as the size of the cluster of lipid molecules bound/absorbed to a protein molecule. This is a very simplified model, but it gives an estimate of the binding reaction parameters, which have been summarized in Table 3. Two measurements over each ratio interval are averaged.

In order to examine the products formed at each titration stage, incubations have also been performed in parallel to the titration experiments. The particle sizes resulting from MLVs are shown as background in Fig. 7 with each lane on the gel corresponding to the ratio represented by the injection. Complexes formed from MLVs and SUVs show a similar size distribution profile.

## 4. Discussion

In this study, we have evaluated conditions needed to give small, homogeneous discoidal rHDL particles, using recombinant apo A-$I_M$ dimer and DMPC vesicles (MLVs and SUVs). The n-PAGE experiments show that the size distribution of complexes is controlled by at least three factors; the ratio, the incubation temperature and the form in which the lipid is presented (i.e. MLV or SUV). The resultant rHDL mixture has been characterized, and the results are discussed based on the model proposed by Jonas et al. (1981) for the formation of rHDL particles, and extended here for the generation of different sized particles from DMPC vesicles and apo A-$I_M$. The first step in this process is considered to be the adsorption of protein to the surface of the vesicles resulting in the formation of lipid-protein vesicular complex. Before the breakdown to small discoidal rHDL particles can take place, sufficient protein must have adsorbed to the vesicle surface. The temperature must also be high enough to provide the energy to induce fragmentation after the protein molecules have adsorbed. In the case of MLVs, the exposed lipid surface area available for the protein is smaller compared to SUV for the same lipid concentration. When the surface of the MLVs are saturated, the protein extracts phospholipid molecules from the outermost shell and forms small rHDL particles. A new bilayer of lipids is now exposed to any un-adsorbed proteins and the process starts again. The protein thus peels off shell after shell of bilayers from the MLVs. In the case of SUVs, the surface area is so much larger that while there may be protein adsorbed to each vesicle, only a few of the vesicle surfaces may have enough proteins adsorbed to induce breakdown into the discoidal rHDL particles. We believe that it may require that the vesicles come in close contact allowing the protein

Table 3
Estimated $K$, $\Delta H$ and $n$ values obtained from the ITC experiments using Eq. (7)

| Ratio (lipid:protein) interval covered by titration | $K$ | | $\Delta H_{app}$ | | $n$ | |
|---|---|---|---|---|---|---|
| | $[M]^{-1}$ | (%) ± | (kJ/mol) | (%) ± | | (%) ± |
| SUV 1700–113 | 1486 | 0 | −5138 | 1 | 700 | 2 |
| MLV 1700–100 | 3067 | 8 | −3143 | 3 | 756 | 3 |
| SUV 3000–200 | 3646 | 32 | −4401 | 10 | 558 | 12 |
| MLV 6000–600 | 2003 | 32 | −4408 | 10 | 1219 | 3 |

molecules to be exchanged between vesicles before saturation can be achieved, thus leading to the subsequent fragmentation. Due to the bilayer curvature and larger number of bilayer defects in SUVs the number of absorbed proteins need not always be the same before fragmentation can start. Hence SUVs result in a more heterogeneous mixture of rHDL particles then MLVs.

The above model is able to explain the observation that incubations with MLVs yield more of the small discoidal rHDL particles than incubations with SUVs at higher temperatures (Fig. 2) since the actual (available) ratio of surface area of lipid to protein in MLV incubations are smaller than in SUV incubations. Furthermore, there will be more SUVs with adsorbed protein, in which the breakdown would not occur, leading to the formation of lipid-protein vesicular complexes. The size of these non-discoidal vesicular complexes will be of the order of SUVs and will not be able to penetrate the n-PAGE gel, leading to staining of protein in the well. Figs. 1 and 2 show that there is nearly always a higher percent protein in 'well' for the SUV incubations than MLVs.

Based on the above model of complex formation, the DSC peaks can be assigned to the various species in the incubation mixture by an examination of the temperatures, enthalpies and trends as a function of ratios. The first transition (peak I) occurs near the transition temperature for multilamellar DMPC and the total enthalpy contained in it is large compared to the others (Fig. 5b). This peak is therefore assigned to the melting of the core-lipids in discoidal complexes and lipids in the lipid–protein vesicular complexes. Of all the lipid molecules in the mixture, a majority exists as part of the core of discoidal complexes with little contact with protein molecules on the surface. Furthermore, these molecules exist as a single bilayer in the disc and will thus not show the high cooperativity of melting as in a multilamellar vesicle. The transition temperature of these lipids will therefore not be significantly affected by the complexation process while the cooperativity of melting will be lowered, resulting in a broad transition as observed in peak I. This broadening and increase in temperature of the main transition has been observed previously (Tall et al., 1977; Edwards et al., 1993). Lipid in the vesicular complexes is also visualized as having a weaker association to the protein, and therefore melts in this peak, further broadening it, especially at the higher ratios.

Examination of the position of peak II in light of the above model suggests that it results from free unassociated protein at the lower ratios, and from weakly associated protein in the lipid-protein vesicular complexes at the higher ratios. Protein in the vesicular complexes also undergoes an increase in its α-helix content (Jonas et al., 1980), leading to a higher cooperativity of the melting process as reflected in the narrower peak II at higher ratios.

Peak III can be assigned to denaturation and melting of the boundary layer of the discoidal complexes and disruption of the H-bonding and van der Waals interactions between the helices and the lipid molecules making up this layer. The decrease in temperature of this peak with increasing ratio (Fig. 5a) may be due to the increasing size of the complex. As the size increases, the average degree of interaction between protein helices and the each boundary layer lipid molecule will decrease resulting in a lowering of degree of stabilization and thereby the melting temperature. This peak has also been similarly assigned by Tall et al. (1977) who suggested that the phospholipid hydrocarbon chains in the boundary layer are stabilized against melting by interaction with the protein. Furthermore, with increasing ratio, a smaller fraction of the total lipid will exist as boundary lipids leading to a decrease in peak III enthalpy when calculated on the basis of total lipid (Fig. 5b).

The observation that a rapid change in the slope of the α-helix-temperature plots (Fig. 6) coincides nicely with the position of peak III in the DSC data, partially confirms the assignment of this peak to a lipid:protein complex. (The CD data cannot however distinguish between protein in discoidal and vesicular complexes). CD also confirms the observation by DSC that the strongly associated boundary layer lipid and protein melt at lower temperatures with increasing ratio (peak III, Fig. 5a), indicating a reduction of

stability. When complexes are heated above the peak III temperature, the discoidal complexes are also disrupted, leading to a release of the core lipids which recombine to form normal vesicles while the protein making up these complexes denatures. Recombination and recomplexation is not completed on cooling within the time scale of the experiment, resulting in the presence of normal DMPC MLV transition peaks on reheating, while peak III decreases in size (Fig. 4b). The lipid does however serve to stabilize the protein at this melting temperature since the loss of a-helicity on heating the complexes is smaller than of the free protein.

The fact that the α-helicity increases as the incubation ratio increases arises from the fact that the particles formed are larger and that with a higher ratio of lipid, more protein molecules bind. Differences in the amount of α-helix in different sized particles and free protein have not been evaluated, but at the higher ratios (200:1 and 100:1) there is no free protein left (Fig. 1). By simple geometric calculations on the smallest formed complexes it is revealed that the 8.2 nm particle can accommodate at the most 14 α-helices (assuming the diameter of one α-helix to be 15 Å), the 10 nm 18, the 11 nm 20 and the 12nm particle 22 α-helices. Since the protein has the ability to form 6, 7 or 8 α-helices, there may be increases in α-helicity instead of binding of more protein molecules. The ability to modify the amount of helices in the protein may also explain the displacement to larger sized complexes with apo A-I compared to apo A-$I_M$. The apo A-I are able to accommodate three protein molecules in each particle while the apo A-$I_M$ which exists as dimer has to have an even number of monomers (two or four).

Another major but less emphasized factor that influences the rHDL particle formation is the temperature dependence of the protein structure itself. As seen in the DSC thermogram, the first protein peak appears at 31°C (Fig. 3b), while the CD data shows a change in the slope at 30°C as the secondary structure decreases (Fig. 6). As the α-helix content decreases, the hydrophobic residues are likely to become more exposed to the solvent, pushing the protein state equilibrium towards the generation of complexes in order to stabilize itself. This driving force towards stabilization of the protein may outweigh the lower reactivity of the lipid itself above the $T_c$, resulting in the observed formation of complex at the high temperatures. The main denaturation peak is 57°C for apo A-I (Gursky and Atkinson, 1996), while 52°C for apo A-$I_M$ and this implies that apo A-$I_M$ would be more reactive than apo A-I at temperatures above lipid melting temperatures. The peak at 30°C seen in DSC for apo A-$I_M$ implies the presence of a low temperature transition, which is not present in apo A-I (Suurkuusk and Hallén, 1998; unpublished results). This may also make the apo A-$I_M$ more reactive at temperatures between 30 and 40°C. The reduction in α-helix content may however also lead to more aggregation of the protein, explaining the larger fraction of unreacted protein in the 40°C MLV incubations (Fig. 2f). The larger available surface area of SUVs may effectively serve to stabilize the protein from self-aggregation, since a larger fraction of the protein may be lipid-surface associated and not available free in solution. This is seen as the smaller amount of free protein in the SUV incubation at 40°C relative to that with MLVs (compare Fig. 2c, 2f). Apo A-I has a higher tendency to self-aggregate due to the lower α-helicity (Calabresi et al., 1994), this implies lower reactivity towards complex formation as seen in Fig. 2f.

Some of the similarities and differences between wild-type apo A-I and apo A-$I_M$ can be understood from the structural studies on these proteins. The structure of the N-terminal part upto the disulfide bridge of apo A-$I_M$ dimer is shown in computer modeling to be similar, but somewhat distorted, to the structure of the N-terminal part of apo A-I in rHDL particles (Calabresi et al., 1997). The occurrence of the disulfide bridge in the C-terminal part, which is considered largely unstructured in lipid-free apo A-I (Laccotripe et al., 1997), causes a structuring of apo A-$I_M$ (Calabresi et al., 1994). The C-terminal in apo A-I is considered important in the initial lipid binding and self-association, and in these events, this part becomes highly α-helical (Davidson et al. 1996; Laccotripe et al. 1997). Apo A-$I_M$ has a

lower tendency to self-associate since the C-terminal may already be stabilized by the interaction of the amphiphatic α-helices between the linked monomers. By mutation studies it is indicated that residues 100–186 are important to the initial association of apo A-I to the lipid surface (Frank et al., 1997), while the C-terminal residues 187–241 are shown crucial for the initial adsorption and penetration into the bilayers (Laccotripe et al., 1997). In order to be able to penetrate the lipid bilayer, the C-terminal adopts a α-helical structure, which might be actually induced by the adsorption step. The adsorption-penetration steps have been recently demonstrated with phospholipid monolayers (Lecompte et al., 1998).

We hypothesize that with apo A-$I_M$ the initial adsorption step might resemble that of apo A-I. However since the C-terminal end of the adsorbing apo A-$I_M$ may already have some degree of structure (Calabresi et al., 1994), the penetration step may be favorable compared to that for apo A-I. Furthermore, in the dimer the C-terminal regions are closely connected tail to tail. When both C-terminals penetrate the lipid bilayer, they may cause more disruption thus facilitating the conversion of vesicle to discs, than the monomeric apo A-I. However, at 25°C no specific difference is seen between apo A-I and apo A-$I_M$, probably due to the temperature being close to the lipid phase transition. At this transition point, the protein insertion is easier due to lattice defects arising between domains of the liquid–crystalline and gel form lipids (Swaney, 1980; Swaney and Chang, 1980). These differences could become more apparent at 40°C, where the lipid is considered unreactive. The reaction of apo A-I with SUVs yields a higher fraction in the well than the reaction with apo A-$I_M$, which might be due to either 'adsorption but no penetration' or 'adsorption and penetration but not enough induced disorder to cause fragmentation'. Apo A-I reactions with MLVs yield larger complexes than apo A-$I_M$, which observation is also explained by the same hypothesized mechanism.

The re-appearance in the DSC thermograms (Fig. 4a) of the second protein peak around 50°C (peak II) when incubating with MLVs at a ratio of 200:1 may also be explained based on the above model. At this and higher ratios, there is not enough protein to cover the full surface of the vesicles as required to induce breakdown into discoidal particles at the incubation temperature at 25°C. This peak II will therefore become increasingly larger with increasing amounts of lipid as more and more protein will exist in this adsorbed state. In the case of incubations with SUVs, the peak is larger compared to that for MLVs (Fig. 5a, Table 1). This follows from the above discussion, and the fact that for the same ratio, SUVs present a larger lipid surface area than MLVs.

Comparing the MLV and SUV incubations shows that the transition temperatures do not differ significantly (Fig. 5a). The enthalpy of the transition involving unassociated or weakly associated lipids (peak I) are affected by the form in which the lipid is presented, while that for the strongly associated complexes (peak III) show no difference (Fig. 5b, Table 1). In all incubations, the total heat of transition (in peaks I + III) is smaller with SUV incubations than in the corresponding MLV incubations. It is well known that the larger curvature of SUVs leads to more defects as well as lesser van der Waals interactions between fatty acid chains, resulting in smaller transition enthalpies compared to MLVs (Kodama et al., 1993). Phospholipid molecules packed in the discoidal complexes are likely to have a higher level of van der Waals interactions resulting in a higher transition enthalpy. The lower total heat of transition in the case of SUVs incubated with proteins thus indicates that at the same lipid to protein ratio, there are less discoidal particles formed from SUVs than from MLVs, in agreement with the above model.

In order to calculate the binding constants from titration data, a model of the binding process has to be set-up. We have however employed a simplified model in this work and the titration data is only being used as a basis for discussion of the lipid binding properties of the protein. The titration experiments span the ratios between 6000:1 to 600:1 at the higher end and 1700:1 to 100:1 at the lower end. A comparison of the microcalorimetric titrations covering ratios 3000:1 to 200:1 (Fig. 7) with the n-PAGE runs (shown in the

background) enables an identification of the type of particles present at each titration step. Based on the model, the first titration injection will yield mostly large particles of lipid–protein vesicular complexes created by the association of the protein with lipid vesicles. This is confirmed by the n-PAGE results, which show that the breakdown of (large) association complexes to (smaller) discoidal particles has not begun to any larger extent at the high ratios. Thus the observed heat flow for the early titrations can be primarily attributed to the association step. With each new injection, as the ratio decreases, increasing amounts of the association complexes will be converted to discoidal particles as confirmed by the n-PAGE results. In parallel, smaller amounts of heat are observed with the increasing ratios. This lends further support to our hypothesis that measured heat is principally due to the association reaction and not an indication of the breakdown of the larger vesicular complexes into the smaller discoidal rHDL particles. This also accounts for the large value of 'n' calculated (Table 3).

Since the association reaction induces conformational changes in the protein as shown by CD, part of the evolved heat is likely to be due to α-helix formation. The enthalpy per residue upon α-helix formation is about −4 kJ/mol (Scholtz et al., 1991). With about 120 amino acids involved in α-helix formation, this accounts for about 10–15% of the total enthalpy. In addition to the α-helix formation, lipids in direct contact with the protein will undergo a phase change from the liquid–crystalline state to the less fluid gel state (Jonas et al., 1980) which is also an exothermic reaction. Another exothermic contribution to the observed enthalpy may arise from the increase in van der Waals interactions upon formation of discoidal complexes, as discussed above. This increase is larger with SUVs than with MLVs, explaining the higher enthalpy for the SUV when titration at the same ratios than with MLVs. Calculating the reaction enthalpy per lipid molecule after first subtracting the estimated α-helix formation enthalpy, yields enthalpies of about −4 and −7 kJ/mol for SUV and MLV lipids respectively. This is of the order of the melting enthalpy of the high temperature peak from the DSC runs, which has been assigned as the melting of boundary lipids. Hence the majority of the observed reaction enthalpy is considered to originate from the protein-induced gel-to-liquid crystalline state transition of boundary lipids. In addition as discussed earlier, it is possible that fragmentation requires insertion of some part of the protein into the lipid bilayer. This process could be either exo- or endothermic as has been shown by peptide titrations to vesicles (Seelig, 1997).

Titration experiments reported earlier have been made at lower ranges of lipid to protein ratios (from 250:1 to 0) (Rosseneu et al., 1974, 1976). They have reported a heat of binding of −1339 kJ/mol with an 'n' value of 132, when titrating to SUVs. Our interpretation of the titration data is supported by a titration study of apo A-I to emulsion particles where no discoidal complexes are formed (Derksen et al., 1996). Derksen et al. thus measured only the energetics of association of apo A-I to the lipid (emulsion) particle surface. The heat of association to the emulsion particles with DPPC on the surface was found to be −3932 kJ/mol of apo A-I. These values lie in the order of the values reported in Table 3 (which are calculated per mol dimer).

## 5. Conclusions

The results of this study suggest that incubation with MLVs at high ratios and temperatures upto 40°C will give a homogenous complex distribution. This will also ensure the absence of uncomplexed protein, but at the cost of an excess of uncomplexed lipid vesicles. However, the size differences between MLVs and the complex can be used to separate them relatively simply by, e.g. centrifugation or ultrafiltration. The exact incubation ratio, temperature and time will need further optimization. The actual choice of lipid has not been addressed in this report. However, from a biological acceptance point of view, DPPC and POPC may be better, although POPC in a formulation will lead to oxidative stability problems.

## Acknowledgements

The authors wish to thank Dr Dan Hallén for valuable discussions.

## References

Andersson, L.-O., 1997. Pharmacology of apolipoprotein A-I. Curr. Opin. Lipidol. 8, 225–228.

Badimon, J., Badimon, L., Fuster, V., 1990. Regression of atherosclerotic lesions by high density lipoprotein plasma fraction in the cholesterol-fed rabbit. J. Clin. Invest. 85, 1234–1241.

Brewer Jr, H.B., Fairwell, T., LaRue, A., Ronan, R., Houser, A., Bronzert, T.J., 1978. The amino acid sequence of human apoA-I, an apolipoprotein isolated from high density lipoproteins. Biochem. Biophys. Res. Com. 80, 623–630.

Calabresi, L., Vecchio, G., Frigerio, F., Vavassori, L., Sirtori, C.R., Franceschini, G., 1997. Reconstituted high-density lipoproteins with a disulfide-linked apolipoprotein A-1 dimer: evidence for restricted particle size heterogeneity. Biochemistry 36, 12428–12433.

Calabresi, L., Vecchio, G., Longhi, R., Gianazza, E., Palm, G., Wadensten, H., Hammarström, A., Olsson, A., Karlström, A., Sejlitz, T., Ageland, H., Sirtori, C.R., Franceschini, G., 1994. Molecular characterization of native and recombinant apolipoprotein A-$1_{Milano}$ dimer. J. Biol. Chem. 269, 32168–32174.

Davidson, W.S., Hazlett, T., Mantulin, W.W., Jonas, A., 1996. The role of apolipoprotein AI domains in lipid binding. Proc. Natl. Acad. Sci. USA 93, 13605–13610.

Derksen, A., Gantz, D., Small, D.M., 1996. Calorimetry of apolipoprotein-A1 binding to phosphatidylcholine–triolein–cholesterol emulsions. Biophys. J. 70, 330–338.

Edwards, W.L., Bush, S.F., Mattingly, T.W., Weisgraber, K.H., 1993. Raman spectroscopic study of boundary lipid in 1,2-dipalmitoylphosphatidylcholine/apolipoprotein A-I recombinants. Spectrochim. Acta 49, 2027–2038.

Fielding, C.J., Fielding, P.E., 1995. Molecular physiology of reverse cholesterol transport. J. Lip. Res. 36, 211–228.

Franceschini, G., Apebe, P., Calabresi, L., Gualandri, V., Sirtori, C.R., 1987. Apolipoprotein A-I, Milano variant: genetic, clinical, and biochemical features. Atherosclerosis Rev. 16, 149–159.

Frank, P.G., Bergeron, J., Emmanuel, F., Lavigne, J.-P., Sparks, D.L., Denèfle, P., Rassart, E., Marcel, Y.L., 1997. Deletion of central α-helices in human apolipoprotein A-I: effect on phospholipid association. Biochemistry 36, 1798–1806.

Glomset, J.A., 1968. The plasma lecithin:cholesterol acyltransferase reaction. J. Lipid Res. 9, 155–162.

Gordon, D.J., Rifkind, B.M., 1989. High-density lipoprotein—the clinical implications of recent studies. N. Engl. J. Med. 321, 1311–1316.

Gursky, O., Atkinson, D., 1996. Thermal unfolding of human high-density apolipoprotein A-I: implications for a lipid-free molten globular state. Proc. Natl. Acad. Sci. USA 93, 2991–2995.

Jonas, A., Drengler, S.M., Kaplan, J.S., 1981. Interaction of apolipoprotein A-I with dimyristoylphosphatidylcholine particles of various sizes. J. Biol. Chem. 256, 2420–2426.

Jonas, A., Drengler, S.M., Patterson, B.W., 1980. Two types of complexes formed by the interaction of apolipoprotein Aa-I with vesicles of l-α-dimyristoylphosphatidylcholine. J. Biol. Chem. 255, 2183–2189.

Kodama, M., Miyata, T., Takaichi, Y., 1993. Calorimetric investigations of phase transitions of sonicated vesicles of dimyristoylphosphatidylcholine. Biochim. Biophys. Acta 1169, 90–97.

Laccotripe, M., Makrides, S.C., Jonas, A., Zannis, V.I., 1997. The carboxyl-terminal hydrophobic residues of apolipoprotein A-I affects its rate of binding and its association with high density lipoprotein. J. Biol. Chem. 272, 17511–17522.

Lecompte, M.-F., Bras, A.-C., Dousset, N., Portas, I., Salvayre, R., Ayrault-Jarrier, M., 1998. Binding steps of apolipoprotein A-I with phospholipid monolayers: adsorption and penetration. Biochemistry 37, 16165–16171.

Meng, Q.-H., Calabresi, L., Fruchart, J.-C., Marcel, Y.L., 1993. Apolipoprotein A-I domains involved in the activation of lecithin:cholesterol acyltransferase. J. Biol. Chem. 268, 16966–16973.

Palguanachari, M.N., Mishra, V.K., Lund-Katz, S., Phillips, M.C., Adeyeye, S.O., Alluri, S., Anantharamaiah, G.M., Segrest, J.P., 1996. Only the two end helixes of eigth tandem amphiphatic helical domains of human apo A-I have significant lipid affinity. Arterioscler. Thromb. Vasc. Biol. 16, 328–338.

Phillips, J.C., Wriggers, W., Li, Z., Jonas, A., Schulten, K., 1997. Predicting the structure of apolipoprotein A-I in reconstituted high-density lipoprotein disks. Biophys. J. 73, 2337–2346.

Pownall, H.J., Hsu, F.J., Rosseneu, M., Peeters, H., Gotto, A.M., Jackson, R.L., 1977. Thermodynamics of lipid protein associations thermodynamics of helix formation in the association of high density apolipoprotein A-I (ApoA-I) to myristoyl phosphatidylcholine. Biochim. Biophys. Acta 488, 190–197.

Rogers, D.P., Brouillette, C.G., Engler, J.A., Tendian, S.W., Roberts, L., Mishra, V.K., Anantharmaiah, G.M., Lund-Katz, S., Phillips, M.C., Ray, M.J., 1997. Truncation of the amino terminus of human apolipoprotein A-I substantially alters only the lipid-free conformation. Biochemistry 36, 288–300.

Rogers, D.P., Roberts, L.M., Lebowitz, J., Engler, J.A., Brouillette, C.G., 1998. Structural analysis of apolipoprotein A-I: effects of amino- and carboxy-terminal deletions on the lipid-free structure. Biochemistry 37, 945–955.

Rosseneu, M., Soetewey, F., Middelhoff, G., Peeters, H., Brown, W.V., 1976. Studies of the lipid binding characteristics of the apolipoproteins from human high density

lipoprotein II. Calorimetry of the binding of Apo AI and Apo AII with phospholipids. Biochim. Biophys. Acta 441, 68–80.

Rosseneu, M.Y., Soetewey, F., Blaton, V., Lievens, J., Peeters, H., 1974. Microcalorimetric study of phospholipid binding to human Apo-HDL. Chem. Phys. Lipid 13, 203–214.

Scholtz, J.M., Marqusee, S., Baldwin, R.L., York, E.J., Stewart, J.M., Santoro, M., Bolen, D.W., 1991. Calorimetric determination of the enthapy change for the α-helix to coil transition of an alanine peptide in water. Proc. Natl. Acad. Sci. USA 88, 2854–2858.

Seelig, J., 1997. Titration calorimetry of lipid–peptide interactions. Biochim. Biophys. Acta 1331, 103–116.

Segrest, J.P., Jones, M.K., DeLoof, H., Brouillette, C.G., Venkatachalapathi, Y.V., Anantharamaiah, G.M., 1992. The amphiphathic helix in the exchangeable apolipoproteins: a review of secondary structure and function. J. Lipid Res. 33, 141–166.

Suurkuusk, M., Singh, S.K., 1998. Microcalorimetric study of the interaction of 1-hexanol with dimyristoylphosphatidylcholine vesicles. Chem. Phys. Lipid 94, 119–138.

Swaney, J.B., 1980. Mechanisms of protein–lipid interaction. J. Biol. Chem. 255, 8791–8797.

Swaney, J.B., Chang, B.C., 1980. Thermal dependence of apolipoprotein A-I–phospholipid recombination. Biochemistry 19, 5637–5644.

Tall, A.R., Small, D.M., Deckelbaum, R.J., Shipley, G.G., 1977. Structure and thermodynamic properties of high density lipoprotein recombinants. J. Biol. Chem. 252, 4701–4711.

Wald, J.H., Krul, E.S., Jonas, A., 1990. Investigation of the lipid domains and apolipoprotein orientation in reconstituted high density lipoproteins by fluorescence and IR methods. J. Biol. Chem. 265, 20044–20050.

Weisgraber, K.H., Rall Jr. S.C., Bersot, T.P., Mahley, R.W., Franceschini, G., Sirtori, C.R., 1983. Apolipoprotein A-$I_{Milano}$. J. Biol. Chem. 258, 2508–2513.